

# Trabecular Bone Radiograph Characterization Using Fractal, Multifractal Analysis and SVM Classifier

I. Slim, H. Akkari, A. Ben Abdallah, I. Bhouiri, M. Hedi Bedoui

**Abstract**—Osteoporosis is a common disease characterized by low bone mass and deterioration of micro-architectural bone tissue, which provokes an increased risk of fracture. This work treats the texture characterization of trabecular bone radiographs. The aim was to analyze according to clinical research a group of 174 subjects: 87 osteoporotic patients (OP) with various bone fracture types and 87 control cases (CC). To characterize osteoporosis, Fractal and MultiFractal (MF) methods were applied to images for features (attributes) extraction. In order to improve the results, a new method of MF spectrum based on the q-structure function calculation was proposed and a combination of Fractal and MF attributes was used. The Support Vector Machines (SVM) was applied as a classifier to distinguish between OP patients and CC subjects. The features fusion (fractal and MF) allowed a good discrimination between the two groups with an accuracy rate of 96.22%.

**Keywords**—Fractal, micro-architecture analysis, multifractal, SVM, osteoporosis.

## I. INTRODUCTION

OSTEOPOROSIS is a silent disease characterized by low bone mass and deterioration of micro-architectural bones, which results in a heterogeneous trabecular bone structure. Any person may have osteoporosis, but it is more frequent in postmenopausal women (50% of women will break a bone due to osteoporosis compared to 25% of men older than 50) [1]. This disease increases the fracture risk since trabecular bones become thin and brittle. The bones of the hip, wrist and vertebral column are the most likely to suffer from fractures due to osteoporosis [2].

Bone Mineral Density (BMD) is an important factor to determine bone fragility [3]. Several works [4], [5], proved that a change of bone characteristic is related not only to BMD but also to the bone micro-architecture structure. An indicator of the bone micro-architecture could allow a better prevention of osteoporosis.

Several studies used the fractal analysis for the discrimination between healthy and osteoporotic groups and they proved that this was a discriminative measure. Authors of [6]-[8] were interested in micro-architecture bone analysis based on Fractal Dimension (FD) which measures the

irregularity of an object. For example, Benhamou et al. [8] applied fractal tools on radiographs of calcaneus for discrimination between healthy and OP groups. Also, Khosrovi et al. [9] applied fractal tools on radiographs of the wrist in osteoporosis diagnosis. In addition, some studies used fractal approaches, such as the fractional Brownian motion [6]-[8] to discriminate between OP patients and healthy ones. A simple FD can be considered as a measure of the degree of complexity of an object. Natural objects or biological ones, as radiographs bone images, are not simple fractals which can be described with a simple FD [10], [11]. Hence, there is a need to use MF analysis, which is an extension of the classical fractal analysis to describe more complex structured objects at different scales [12].

In this study, we are interested in the diagnosis of osteoporosis using Fractal and MF methods. These techniques are applied on radiographs images to extract features (Fractal and MF attributes). The Differential Box Computing (DBC) method was used to estimate the FD. Moreover, a new MF spectrum based on the q-structure functions was proposed and it is used to extract the MF attributes, i.e. the minimum singularity coefficient ( $\alpha_{\min}$ ), the maximum singularity coefficient ( $\alpha_{\max}$ ) and the area under spectrum (AUS). The SVM was used as classifiers to distinguish between OP patients and CC subjects. This paper is organized as follows: sections 2 and 3 details respectively, the DBC method used to calculate the FD and the MF spectrum calculation based on the q-structure functions are detailed. Sections 4 and 5 include the used database and the proposed methodology. The results are illustrated in section 6. Finally, in section 7 and 8, a discussion and some perspectives conclude this paper.

## II. FRACTAL ANALYSIS: DIFFERENTIAL BOX-COUNTING METHOD (DBC)

The main advantage of the DBC is the use of grayscale images. It considers an image as a three-dimensional object, where  $(x, y)$  are the coordinates of its pixel and  $z$  is its gray level [13]. The space  $(x, y, z)$  is divided into cubes of size  $(\varepsilon \times \varepsilon \times \varepsilon)$ . For each window  $f(i, j)$  of size  $(\varepsilon \times \varepsilon)$  of the plane  $(x, y)$ , the number,  $L$  of the box containing the maximum gray level and the number,  $k$  of the box with the minimum gray level are determined, according to (1):

$$n_r = L - k + 1 \quad (1)$$

where  $r = \varepsilon / M$  for an image, sized  $(M \times M)$  and  $n_r$  is the number of boxes sized  $(\varepsilon \times \varepsilon \times \varepsilon)$  required to contain the

I. Slim is a PhD student, H. Akkari and A. Ben Abdallah are doctors with the Laboratory of Technology and medical imagery LTIM-LR12ES06, Faculty of Medicine, Monastir, Tunisia (corresponding author, e-mail: slim\_ines5@yahoo.fr, hanen.bettaieb@gmail.com, assoumaba@yahoo.com).

I. Bhouiri is a professor with the Research Unit wavelet and multifractal, Faculty of science, Monastir, Tunisia (e-mail: bhouiri\_imen@yahoo.fr).

A. Bedoui is a professor with the Laboratory of Technology and medical imagery LTIM-LR12ES06, Faculty of Medicine, Monastir, Tunisia (e-mail: medhedi.bedoui@fmm.rnu.tn\ hedi.bedoui2015@gmail.com).

portion of the surface in the corresponding window  $f(\varepsilon \times \varepsilon)$ , with  $\varepsilon \in [2, M/2]$ . The FD is obtained using (2) and  $N$  is the sum of  $n_r$  in all windows:  $N = \sum_{i,j} n_r(i, j)$ ,  $(i, j)$  are the coordinates of a window  $f$ . The FD is given by:

$$FD = \lim_{\varepsilon \rightarrow 0} \left( \frac{\log(N(\varepsilon))}{\log\left(\frac{1}{\varepsilon}\right)} \right) \quad (2)$$

### III. THE MF ANALYSIS BASED ON THE Q-STRUCTURE FUNCTION

The spectrum calculation is based on the q-structure functions [14] as a partition function. The q-structure function is used to study the grayscale variation along a set of pixels included in the image for different scales  $\varepsilon$ . It allows the regularity analysis of an object [14].

The discrete q-structure function  $S_q$  is defined as [14]:

$$S_q(\varepsilon) = \left( \varepsilon \times \sum_t |f(t+\varepsilon) - f(t)|^q \right)^{\frac{1}{q}}, \quad q \neq 0 \quad (3)$$

$$S_0(\varepsilon) = \varepsilon \times \sum_t |f(t+\varepsilon) - f(t)|, \quad q = 0 \quad (4)$$

where  $t$  is the position of a pixel from the image,  $f(t)$  is the gray level of the pixel  $t$ ,  $q$  is a moment, and  $\varepsilon$  is the scale.

The multi-scale function  $\tau_N$  associated to rugosity exponents of the function  $f$  at different scales  $\varepsilon = \frac{1}{2^N}$  is defined by the function  $\tau_N(q): q \in \mathbb{R} \rightarrow \tau_N(q)$  with:

$$\tau_N(q) = q - q \left( \frac{\log(S_q)}{\log \varepsilon} \right), \quad q \neq 0 \quad (5)$$

$$\tau_N(q) = 0, \quad q = 0 \quad (6)$$

and

$$\tau(q) = \lim_{N \rightarrow \infty} \tau_N(q) \quad (7)$$

$\tau(q)$  presents the global characterization of singularity of the function  $f$ . In addition, we can characterize the local measure by:

$$\alpha(q) = \frac{d\tau(q)}{dq} \quad (8)$$

$\alpha(q)$  is called the local regularity coefficient and it will be used as MF attributes to study radiographs images. The MF

spectrum  $f^*$  is defined by:

$$f^*(\alpha(q)) = \alpha(q) \times q - \tau(q), \quad q \in \mathbb{R} \quad (9)$$

### IV. MATERIAL

Our database is composed of 174 trabecular bone radiograph images of postmenopausal women. These images are sized (400×400) pixels with 100  $\mu\text{m}$  resolution and obtained on calcaneus (bone of the heel) with a numeric prototype of X-ray [15]. There were 87 controls (CC) and 87 patients with osteoporotic fractures (OP). Among the OP subjects, there were 21 patients with hip fracture (HF), 22 with vertebral fracture (VF), 23 with wrist fracture (WF) and 21 with other fracture (OF). Since age and number of fractures have an influence on bone density and on trabecular bone texture, the fracture cases ( $71.3 \pm 10.5$  years) were age-matched with the CC cases ( $70.1 \pm 10.2$  years). Moreover, the number of fractures for each patient is known.

### V. METHODOLOGY

In order to discriminate between OP patients and CC cases, the DBC method and the new MF spectrum were applied on the trabecular bone radiograph images: the CC group and the OP group with various fracture types. For classification, the used features were the FD obtained from the DBC method and three attributes deduced from the MF spectrum based on the q-structure functions. These are the minimum singularity coefficient ( $\alpha_{\min}$ ), the maximum singularity coefficient ( $\alpha_{\max}$ ) and the area under the spectrum noted 'AUS'.

Finally, to evaluate and compare the effectiveness of the different attributes, we used the SVM. It is one of the most popular supervised classifiers in machine learning and pattern recognition.

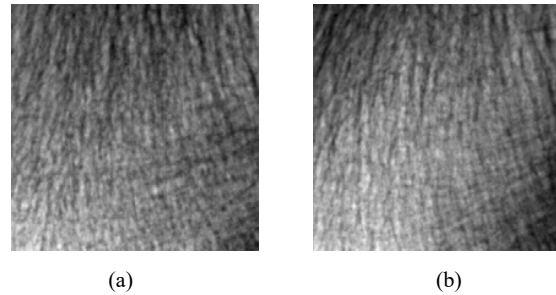


Fig. 1 Trabecular bone radiographs image, (a) control patient (b) OP

The SVM classification was achieved by constructing a hyperplane that optimally discriminated the data into two classes [16]. For real data like medical images, the non-linear classification is very useful. For this reason, we choose the SVM classifier and based on the kernel functions, the non-linear classification can be used. The SVM classifier [17], [18] was trained using a training set that contained bone radiograph images from the CC group and the OP patients. The performance of the classifier was checked using the RBF

kernel. There was no overlap between the images used for training and testing.

Fig. 1 presents two radiographs images from our database; Fig. 1 (a) image of control patient, Fig. 1 (b) image of an OP. As it is shown, that is very difficult to discriminate between the two images.

Fig. 2 shows an example of a MF spectrum based on the q-structure function. The MF attributes deduced from it are:  $\alpha_{\min} = 12.81$ ,  $\alpha_{\max} = 19.52$  and  $AUS = 59.79$ .

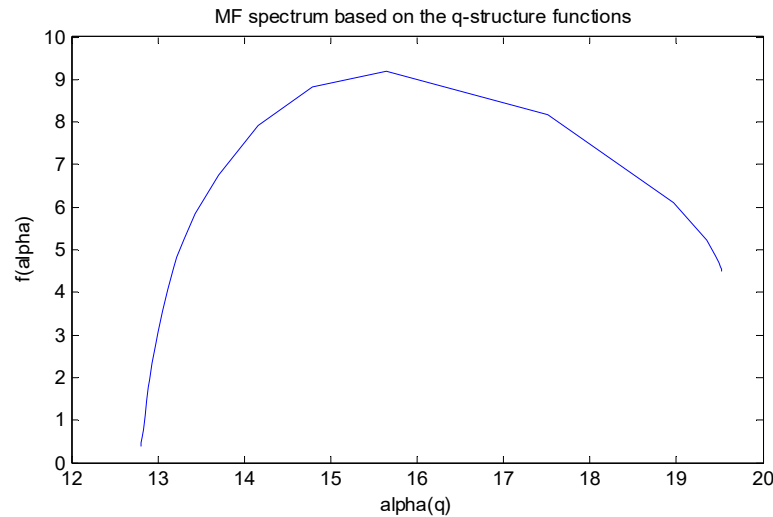


Fig. 2 The MF spectrum based on the q-structure functions

$$Accuracy = \frac{TP + TN}{TP + FP + TN + FN} \quad (10)$$

where: True Positive (TP) is the number of osteoporotic people correctly identified. False Positive (FP) is the number of healthy people incorrectly identified. True Negative (TN) is the number of healthy people correctly identified. False Negative (FN) is the number of osteoporotic people incorrectly identified.

In order to distinguish between the two groups, we firstly used each FD and MF attribute ( $\alpha_{\min}$ ,  $\alpha_{\max}$  or AUS), then we used these features combined. The number of fracture of each patient is known and used for the classification.

#### A. Results Obtained by Each Method

Table I shows the classification rate found for different classifications performed with each attribute separately.

The results show that the DBC method discriminates all OP people with different types of fractures from healthy ones with an accuracy rate of 42.16% and also allows the classification of the two groups with the MF attributes with better scores. In fact, we obtained a classification rate of 78.31%, 79.51%, and 80.72%, respectively for using the  $\alpha_{\max}$ , the  $\alpha_{\min}$  and the AUS. In addition, results of the discrimination between the CC group and the different fracture groups with the MF attributes ( $\alpha_{\max}$ ,  $\alpha_{\min}$  and AUS) show better classification rates, especially for Hip fractures where we obtained a classification rate of 93.79%, 93.56% and 84.56% respectively for using the  $\alpha_{\max}$ , the  $\alpha_{\min}$  and the AUS. For the other fracture types,

## VI. RESULTS

The Fractal and MF measures were applied on the trabecular bone radiograph images: the CC group and the OP one with various fracture types: HF, VF, WF and OF. The SVM with the RBF kernel was used as a classifier to distinguish between two populations and the effect of the different attributes was estimated based on the accuracy rate defined by (10).

acceptable scores were achieved.

TABLE I  
ACCURACY RATE OF SEVERAL CLASSIFICATIONS USING EACH ATTRIBUTE

|                 | FD     | $\alpha_{\min}$ | $\alpha_{\max}$ | AUS     |
|-----------------|--------|-----------------|-----------------|---------|
| HF vs. CC       | 90.56% | 93.79%          | 93.56%          | 84.56%  |
| VF vs. CC       | 90.56% | 90.56%          | 90.56%          | 83.189% |
| WF vs. CC       | 90.56% | 90.56%          | 90.56%          | 73.58%  |
| OF vs. CC       | 96.22% | 90.56%          | 90.56%          | 83.18%  |
| Total OP vs. CC | 42.16% | 79.51%          | 78.31%          | 80.72%  |

#### B. Results with Combined Attributes

Table II shows the classification rates found for different classifications performed using the combination of the FD and the MF attributes.

TABLE II  
ACCURACY RATE OF SEVERAL CLASSIFICATIONS USING THE COMBINATION OF THE DIFFERENT ATTRIBUTES

|                 | FD and $\alpha_{\min}$ | FD and $\alpha_{\max}$ | FD and AUS |
|-----------------|------------------------|------------------------|------------|
| HF vs. CC       | 96.22%                 | 96.22%                 | 94.76%     |
| VF vs. CC       | 94.33%                 | 94.33%                 | 87.53%     |
| WF vs. CC       | 94.33%                 | 94.33%                 | 79.24%     |
| OF vs. CC       | 94.33%                 | 94.33%                 | 91.53%     |
| Total OP vs. CC | 60.84%                 | 57.83%                 | 59.03%     |

Table II shows the classification rate of the discrimination between CC and the OP groups with various fracture types: HF, VF, and WF and OF using the combination of the FD

with each MF attribute. The results in Table II show an improvement of the accuracy rate for different performed classifications. We have specially obtained excellent classification rates of 96.22%, 96.22%, and 94.76% for the discrimination between the CC group and the Hip fracture group respectively for the combination of (FD and  $\alpha_{\min}$ ), (FD and  $\alpha_{\max}$ ) and (FD and AUS). Also, the features fusion enhanced results for the different fracture types (VF, WF and OF) with good scores.

## VII. DISCUSSION

This paper proposes the application of FD estimated by the DBC method and the MF spectrum based on the q-structure functions. These techniques were used to analyze trabecular bone radiograph images and discriminate between a healthy group and an osteoporotic one. The advantage of the DBC method is that it can be applied on grayscale images and it allows the irregularity description of an object. The MF spectrum based on the q-structure function is able to evaluate the local and global regularity, which can be very helpful for the micro-architecture analysis and precisely for radiograph images analysis. The originality of this work is the combination of fractal and MF attributes for the diagnosis of osteoporosis.

In Table I, the results show that the MF attributes present better classification rates than those found with the DBC for all types of fractures. We can conclude that the MF attributes are more discriminate than the FD. Since the MF spectrum is able to describe both the local and global irregularities of an image, it shows better classification rates. The results in Table II show pertinent classification rates for the discrimination between the CC group and the Hip fracture group. This result may be related to the fact that people affected by this type of fracture are very likely to have osteoporosis. This score was not found with other types of fractures (vertebral, wrist) which are probably present in osteopenic patients. Compared with the results found in [7], for the same database of images, the combination of the FD calculated with the DBC method and the MF attributes deduced from the MF spectrum is able to better characterize trabecular bone images without any pre-treatment. In fact, the fusion of FD and MF attributes improved the classification score of hip fractures from 85% to 96.22% with using (FD and  $\alpha_{\max}$ ). Also, our approach discriminated all the other fracture types (VF, WF and OF) with good rates which could not be reached in [7].

## VIII. CONCLUSION

In this study, a new approach of MF spectrum calculation based on the q-structure function was proposed. It is combined with the DBC method and applied on trabecular bone radiograph images.

The aim of this work was to analyse the micro-architecture bone in order to discriminate between patients with osteoporosis with various fracture types and controls. The obtained results show various successful and improved score classifications compared to [7], [19]. The combination of

fractal and MF attributes presents a good tool to describe and evaluate the non-uniform distribution phenomenon.

To complete this study, we propose to use a larger database. Also, we put forward to apply this approach on another trabecular bone database image with osteopenic patients in order to improve osteoporosis prevention.

## REFERENCES

- [1] <https://www.nlm.nih.gov/medlineplus/osteoporosis.htm>. Accessed on: 08/10/2017.
- [2] [http://www.passeportsante.net/fr/Maux/Problemes/Fiche.aspx?doc=osteoporose\\_pm](http://www.passeportsante.net/fr/Maux/Problemes/Fiche.aspx?doc=osteoporose_pm). Accessed on: 15/09/2017.
- [3] A. Consensus. Consensus development conference: diagnosis, prophylaxis, and treatment of osteoporosis. *Am J Med*, 94(6):646–50, 1993.
- [4] J. S. Bauer and T. M. Link. Advances in osteoporosis imaging. *European journal of radiology*, 71(3):440–449, 2009.
- [5] E. Lespessailles, C. Chappard, N. Bonnet, and C. L. Benhamou. Imaging techniques for evaluating bone microarchitecture. *Joint Bone Spine*, 73(3):254–261, 2006.
- [6] K. Harrar, L. Hamami, E. Lespessailles, and R. Jennane. Piecewise whittle estimator for trabecular bone radiograph characterization. *Biomedical Signal Processing and Control*, 8(6):657–666, 2013.
- [7] Tafrouti, A., El Hassouni, M., Toumi, H., Lespessailles, E., & Jennane, R. (2014, November). Osteoporosis Diagnosis Using Fractal Analysis and Support Vector Machine. In *Signal-Image Technology and Internet-Based Systems (SITIS)*, 2014 Tenth International Conference on (pp. 73-77). IEEE.
- [8] Benhamou C, Lespessailles E, Jacquet G, Harba R, Jennane R, Loussot T, et al. Fractal organization of trabecular bone images on calcaneus radiographs. *J Bone Miner Res* 1994;9:1909–18.
- [9] Khosrovi P, Kahn A, Genant H, Majumdar S. Characterization of trabecular bone structure from radiographs using fractal analysis. Sixteenth Annual Meeting of the American Society for Bone and Mineral Research. Kansas City, Missouri; 1994: S156.
- [10] D. L. Ruderman and W. Bialek. Statistics of natural images: Scaling in the woods. *Physical review letters*, 73(6):814–817, 1994.
- [11] D. L. Ruderman. Origins of scaling in natural images. *Vision research*, 37(23):3385–3398, 1997.
- [12] J. L. Veהל. Introduction to the multifractal analysis of images, 1998.
- [13] Chaudhuri, B. B., & Sarkar, N. (1995). Texture segmentation using fractal dimension. *Pattern Analysis and Machine Intelligence*, IEEE Transactions on, 17(1), 72-77. <http://dx.doi.org/10.1109/34.368149>
- [14] C. Tricot. A model for rough surfaces. *Composites science and technology*, 63(8):1089–1096, 2003.
- [15] E. Lespessailles, C. Gadois, I. Kousignian, J. Neveu, P. Fardellone, S. Kolta, C. Roux, J. Do-Huu, and C. Benhamou. Clinical interest of bone texture analysis in osteoporosis: a case control multicenter study. *Osteoporosis international*, 19(7):1019–1028, 2008.
- [16] N. Cristianini and J. Shawe-Taylor, *An Introduction to Support Vector Machines and Other Kernel-based Learning Methods*, 1st ed. Cambridge University Press, 2000.
- [17] C.C. Chang, C.J. Lin, LIBSVM: A library for support vector machines. 2001. <http://www.csie.ntu.edu.tw/~cjlin/libsvm>. Accessed on: 20/09/2017.
- [18] S. S. Keerthi, S. K. Shevade, C. Bhattacharyya, K. R. K. Murthy, Improvements to platt's SMO algorithm for SVM classifier design, *Neural Comput*.13 (2001) 637–649.
- [19] R. Jennane, J. Touvier, M. Bergounioux, and E. Lespessailles. A variational model for trabecular bone radiograph characterization. In *Biomedical Imaging (ISBI)*, 2014 IEEE 11th International Symposium on, pages 1283–1286. IEEE, 2014.